

Observation of Photovoltaic Effect and Single-photon Detection in Nanowire Silicon pn-junction

Arief Udhiarto^{1,2*}, Sri Purwiyanti^{1,2}, Daniel Moraru¹, Takeshi Mizuno¹, and Michiharu Tabe¹

1. Research Institute of Electronics, Shizuoka University, 3-5-1 Johoku, Naka-ku, Hamamatsu 432-8011, Japan
2. Electrical Engineering Department, Faculty of Engineering, Universitas Indonesia, Depok 16424, Indonesia

*E-mail: arief@shizuoka.ac.jp

Abstract

We study nanowire silicon pin and pn-junctions at room and low temperature. Photovoltaic effects are observed for both devices at room temperature. At low temperature, nanowire pn-junction devices show their ability to detect single photon. This ability was not been observed for pin devices. Phosphorus-boron dopant cluster in the depletion region is considered to have the main role for single-photon detection capability. Fundamental mechanism of dopant-based single-photon detection in nanowire pn-junction is described in details.

Abstrak

Pengamatan terhadap Efek Fotovoltaik dan Deteksi Foton Tunggal pada Simpangan-pn Silikon Kawat Nano. Kami mempelajari pin dan simpangan-pn silikon pada suhu ruangan dan suhu rendah. Efek fotovoltaik diamati pada kedua komponen pada suhu ruangan. Pada suhu rendah, komponen simpangan-pn kawat nano menunjukkan kemampuan untuk mendeteksi adanya foton tunggal. Kemampuan ini tidak ditemukan pada komponen pin. Kluster dopan boron berfosfor pada daerah deplesi dianggap memainkan peranan utama dalam kemampuannya untuk mendeteksi foton. Mekanisme dasar dari deteksi foton tunggal berbasis dopant pada simpangan-pn kawat nano digambarkan secara mendetail.

Keywords: dopant cluster, nanowire pn-junction, single dopant, single photon

1. Introduction

Current fabrication technology has provided an ability to build device structures with quasi-atomic precision. Well-known fundamental microelectronic devices, such as transistor and diode, have been miniaturized into nanoscale size. In this nanoscale regime, the behavior of devices is found to be drastically modified as compared to their bulk counterparts. In addition to the quantum size effect, which is commonly considered as the origin behind nanoscale phenomena [1], random dopant distribution has been reported as another source behind the changing in device performance [2–4]. More importantly, it has been reported that individual donor [5–6] and acceptor [7–8] may mediate carrier transport. This has opened an opportunity to utilize individual dopant as an active part for device functionalities. As an individual entity, dopant has unique properties, such as discrete electronic states, neutral and ionized, which suggests that it may work as a switch. Due to its localized potential, a dopant has been considered as a

natural atomic quantum dot. Based on these unique properties, some groups are working to realize dopants based devices [9–10]. Several examples such as dopant based quantum computing [11–12], single-dopant turnstile [13–14], single-dopant transistors [15], single-dopant memory [16], and single-dopant based single-photon detection [17], have been proposed [18]. Most of these devices are based on metal-oxide-semiconductor field-effect-transistors (MOSFET) structure, in which operation relies only on one type of dopant. For photonics application, such as solar cell and photon detection devices, pn junction and pin diode structure are more commonly used. So far, the behavior of nanoscale pn-junction has been also reported [19–20]. The effect of individual dopants and their interaction with photons in pn-junction structure, however, have not been yet clarified. In this paper, focusing on the effect of individual dopants, we study the nanowire pin and pn-junction at room and low temperatures, in dark and under light illumination.

2. Methods

We fabricated and studied two types of nanowire junction diode, pn and pin. Schematic device structure, bias configuration and schematic top view for both devices are shown in Fig. 1. The nanowire was patterned on silicon-on-insulator (SOI) structure using electron beam lithography. The width, length, and thickness are estimated to be 15, 1000, and 5 nm, respectively. Boron and phosphorus atoms were selectively diffused to create lateral pn-junction and pin devices. In pn-junction devices, a co-doped region was doped with phosphorus and boron simultaneously. Boron concentration is higher than phosphorus concentration. For both devices, final phosphorous and boron concentration derived from secondary ion mass spectrometry (SIMS) are estimated to be $N_D \approx 1 \times 10^{18} \text{ cm}^{-3}$ and $N_A \approx 1.5 \times 10^{18} \text{ cm}^{-3}$ respectively. In the pin devices, an area in the middle part of the nanowire was kept un-doped. The nanowire is covered with a 10-nm-thick SiO_2 layer. The p-Si substrate was doped with boron ($N_A \approx 1.5 \times 10^{15} \text{ cm}^{-3}$) and used as a gate. The thickness of the buried oxide layer is 150 nm.

Devices were measured in a vacuum chamber of an electrical measurement system. p-type region was connected to the voltage source, while n-type region and substrate were kept grounded. Light is illuminated onto the device from a halogen or a monochromatic light source in the visible wavelength range is connected with optical fibers through a quartz window. The illumination area in the device has a diameter of about 3.2 mm. By dividing the measured optical power at the sample surface over the illumination area and the photon energy, the incident photon flux is estimated.

3. Results and Discussion

Room temperature measurement. We measured the anode current versus applied voltage ($I-V_A$) characteristics at room temperature; substrate (V_{Sub}) was kept constant at 0 V, while V_A was swept from negative to positive values. Figure 2 shows typical $I-V_A$ characteristics for pin (a) and pn-junction (b) in dark and under halogen light illumination for several incident photon fluxes (Φ_{inc}), increasing from top to bottom. For both devices, photovoltaic effect can be clearly observed. It is well known that photovoltaic effect in pn-junction is observed as an increase of the current in the negative direction at zero or reversed bias condition under light illumination. Even though both devices show photovoltaic effect, apparently some differences can be observed. Under the same Φ_{inc} , in the reversed bias region, pn-junction shows higher current as compared to the pin-junction device. In the larger forward bias region, pn-junction devices also show strong dependence on Φ_{inc} , therefore, a crossing point is clearly observed at a bias around 0.3 V [Fig. 2 (b)]. On

the other hand, pin-junction devices show weaker dependent on Φ_{inc} , therefore the cruces almost merge at higher bias.

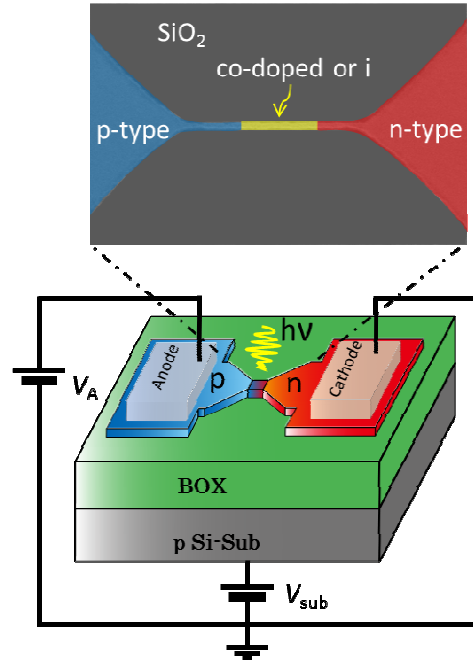


Fig. 1. Schematic Device Structure, Bias Configuration and Schematic Top View of pn-junction Area

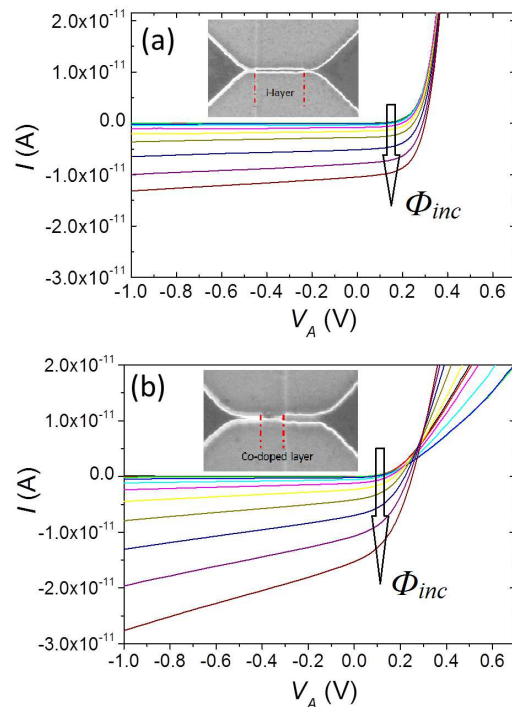


Fig. 2. Typical $I-V_A$ Characteristics of (a) Pin-devices and (b) pn-junction Devices. Both Devices Show Photovoltaic Effect under Halogen Light Illumination. Inset: SEM Images

It is unexpected that pn-junction has higher sensitivity to the Φ_{inc} as compared to the pin-junction devices. It is known that pin-junction structure is commonly used as a photodetector since it can optimize the quantum efficiency [21]. The reason why our pn-junction devices are more sensitive to photons than the pin-junction devices most likely comes from the fact that pn-junction device has final width and thickness narrower and thinner than pin-junction devices. This is due to additional consumption of silicon by the double doping process in the co-doped region. The difference can be seen from scanning electron microscope (SEM) images as shown in the inset of Fig. 2. Based on these images, the origin of the photocurrent enhancement can be ascribed as follows.

Since co-doped layer is narrower and thinner, the resistivity increases and nanowire becomes insulator-like. When a voltage bias is applied, the potential is tilted as schematically shown in Fig. 3. In the forward bias, electrons and holes can easily diffuse as indicated by thick arrows. Under light illumination, additional electrons and holes are generated in the entire nanowire. A small number of electrons and holes are generated in the depletion region and immediately drifted in the opposite direction (thin arrows) from the main diffusion current; therefore, the main current is reduced, as generally reported for conventional pn-junction. A larger number of carriers, however, are generated in the tilted potential region. The photogenerated electrons in this area flow from n-type to p-type and enlarge the main diffusion current. As a result, higher current is observed for higher light intensity. In the reverse bias, similar results are observed as well due to similar mechanism.

Low temperature measurement. At room temperature, we observe the photovoltaic effect which is normally observed for bulk pn-junction devices. Effect of individual dopants has not been observed at this temperature regime. In order to observe the effect of individual dopants, we need to suppress the carrier's thermal energy. For that purpose, we lowered the

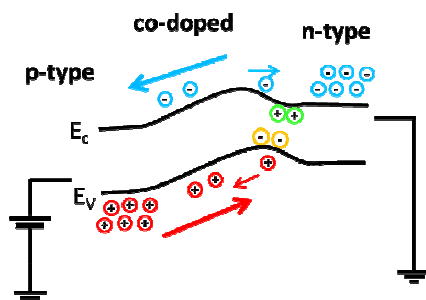


Fig. 3. Schematic Band Diagram of Nanowire pn-junction and Carrier Flow under Light Illumination. More Photogenerated Electrons and Holes Enhance the Main Current Due to Tilted Effect

temperature measurement down to ~ 20 K ($\sim -250^\circ$ C). At this temperature regime, most dopants are freeze-out and the density of free carriers is drastically reduced [22]. I - V_A characteristics in the forward bias for pin and pn-junction devices at this temperature are shown in Fig. 4(a) and 4(b) respectively.

Compared with room temperature measurement, higher voltage bias is required to obtain the same current level. In our experiment, around 5 V is required for pin device, in dark, to reach the threshold voltage, which is much higher, compared to room temperature (below 0.5 V).

Higher voltage is necessary since most of the applied voltage is dropped beyond the junction region due to freeze-out effect. Under light illumination, some electrons and holes are generated providing additional free carriers. As free carriers increase, conductivity is enhanced; therefore, lower voltage is required to reach the same current level. For pn-junction device, similar results are observed for dark condition. Under light illumination, however, current exhibits noise features as shown in Fig. 4(b).

In order to observe this noise feature, we performed current versus time (I -time) measurement for a constant V_A , in dark and under monochromatic light ($\lambda = 410$ nm) for several Φ_{inc} . Figure 5 shows I -time in dark and under several Φ_{inc} (increasing for bottom to top). In dark, current is almost constant without any significant fluctuation. Under light illumination, current switches between two or more current levels and is observed as

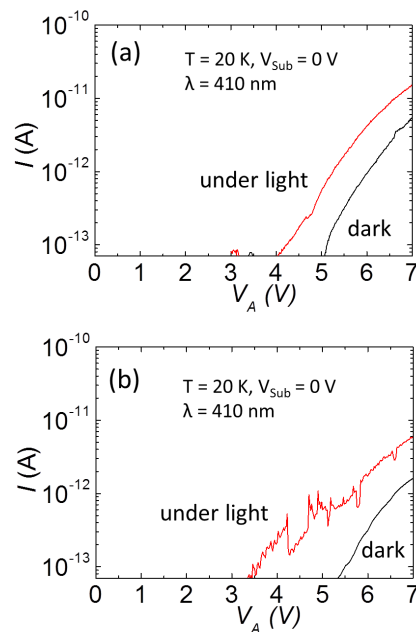


Fig. 4. Low Temperature I - V_A Characteristics of (a) Pin-devices and (b) pn-junction Devices. Only pn-junction Devices Show Noise Feature under Light Illumination

random telegraph signal (RTS). Number of RTS monotonically increases by increasing Φ_{inc} , indicating that RTS is triggered by photons. These results are direct evidence of single-photon detection. Detailed detection mechanism can be described as follows.

Since RTS, as signature of single-photon detection, are only observed for pn-junction devices, this indicates that phosphorus-boron cluster in the co-doped region plays an important role. Due to the random dopants distribution, a phosphorus dopant may accidentally be surrounded by boron dopants, creating a volcano-like shape, as schematically shown in Fig. 6(a). Ionized phosphorous dopant is shown as crater surrounded by boron dopant potential. When a forward biased voltage is gradually applied, potential barrier in the depletion region is reduced. It allows electrons and holes to flow in the opposite direction as diffusion current. For simplicity, we will focus on the electron current, shown by dotted arrow, which flows from n-type (right) to p-type (left) region.

The density of diffusion electrons is strongly dependent on temperature and applied voltage. At low temperature and small forward bias, density of diffusion electrons is strongly suppressed. Only a few electrons can overcome the potential barrier and flow to the p-type region through the lowest potential region. In dark, the diffusion electrons, however, cannot overcome the hill created by boron dopants to neutralize the ionized phosphorus dopant, as far as the applied voltage and temperature are kept constant. Therefore, the measured current must be constant, as experimentally shown in Fig. 5.

When photons with energy higher than energy band gap are absorbed in the nanowire, electrons and holes are generated. The photoexcited electron will immediately lose its energy due to phonon emission [23] and can be

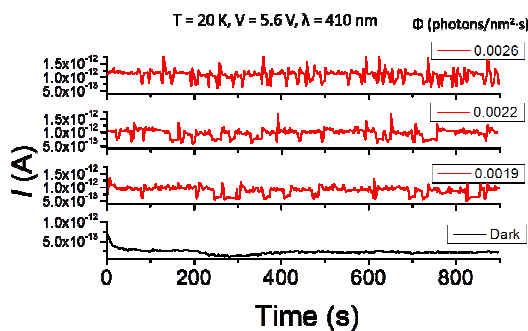


Fig. 5. *I*-time Characteristics in Dark and under Light Illumination. Under Light Illumination, Current Switch between Two or More Levels as Random Telegraph Signal (RTS). By Increasing Photon Flux (Φ), from Bottom to Up, Number of RTS Increases, Suggesting that RTS is Triggered by Photons

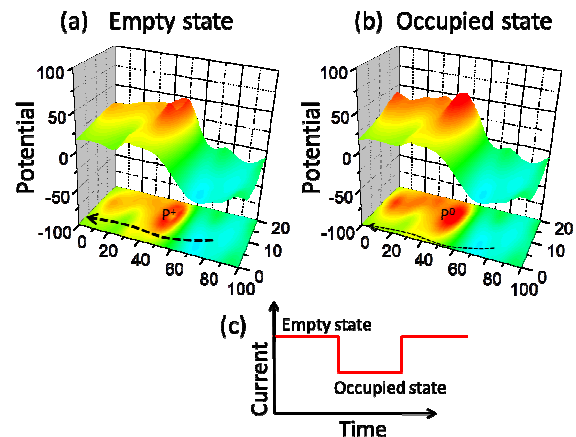


Fig. 6. Schematic of Simulated Potential Landscape of Nanowire pn-junction in the Depletion Region. A Phosphorus Dopant is Accidentally Surrounded by Boron Dopants. (a) Phosphorus Dopant is Ionized, Creating Volcano Shape Like. (b) Phosphorus Dopant is Neutral Causing Increase in the Potential, Reducing the Current

captured by the ionized phosphorus dopant. Once the phosphorus dopant is neutralized, its potential rises. This causes the sudden rise of potential in the depletion region, reducing the diffusion current, as schematically illustrated in Fig. 5(b). Since electric field exists in the depletion region, the trapped electron will quickly escape and phosphorus dopant is ionized. As a result, the depletion region potential returns to the initial condition as well as the current. Based on these events of trapping and detrapping of photoexcited electrons, sudden current changes are observed as random telegraph signal (RTS), as shown in Fig. 5(c).

4. Conclusions

We demonstrated the photovoltaic effect in silicon nanowire pin and pn-junction. pn-junction devices generate more power compared to pin-junction devices due to their smaller dimension. pn-junction devices show their ability to detect single photon, taking advantage of the random phosphorus-boron distribution. These results may give an insight for future nanophotonics devices.

References

- [1] T. Hiramoto, H. Majima, M. Saitoh, Mater. Sci. Eng. B. 101/1-3 (2003) 24.
- [2] A. Asenov, IEEE T. Electron. Dev. 45/12 (1998) 2505.
- [3] T. Shinada, S. Okamoto, T. Kobayashi, I. Ohdomari, Nature. 437/7062 (2005) 1128.
- [4] M. Hori, T. Shinada, Y. Ono, A. Komatsubara, K. Kumagai, T. Tani, T. Endoh, I. Ohdomari, Appl. Phys. Lett. 99/6 (2011) 062103.

- [5] H. Sellier, G. P. Lansbergen, J. Caro, N. Collaert, I. Ferain, M. Jurczak, S. Biesemans, S. Rogge, *Phys. Rev. Lett.* 97/20 (2006) 206805.
- [6] G.P. Lansbergen, R. Rahman, C.J. Wellard, I. Woo, J. Caro, N. Collaert, S. Biesemans, G. Klimeck, L.C.L. Hollenberg, S. Rogge, *Nat. Phys.* 4/8 (2008) 656.
- [7] Y. Ono, K. Nishiguchi, A. Fujiwara, H. Yamaguchi, H. Inokawa, Y. Takahashi, *Appl. Phys. Lett.* 90/10 (2007) 102106.
- [8] M.A.H. Khalafalla, Y. Ono, J. Noborisaka, G.P. Lansbergen, A. Fujiwara, *J. Appl. Phys.* 110/1 (2011) 014512.
- [9] P.M. Koenraad, M.E. Flatté, *Nature Materials*. 10/2 (2011) 91.
- [10] D. Moraru, A. Udhiarto, M. Anwar, R. Nowak, R. Jablonski, E. Hamid, J.C. Tarido, T. Mizuno, M. Tabe, *Nanoscale Res. Lett.* 6 (2011) 479.
- [11] H.-S. Goan, *Quantum Information Science - Proceedings of the 1st Asia-Pacific Conference*, 393/6681 (2005) 27.
- [12] L. Hollenberg, A. Dzurak, C. Wellard, A. Hamilton, D. Reilly, G. Milburn, R. Clark, *Phys. Rev. B.* 69/11 (2004) 113301.
- [13] D. Moraru, Y. Ono, H. Inokawa, M. Tabe, *Phys. Rev. B.* 76/7 (2007) 075332.
- [14] D. Moraru, M. Ligowski, K. Yokoi, T. Mizuno, M. Tabe, *Appl. Phys. Express.* 2 (2009) 071201.
- [15] M. Tabe, D. Moraru, M. Ligowski, M. Anwar, R. Jablonski, Y. Ono, T. Mizuno, *Phys. Rev. Lett.* 105/1 (2010) 016803.
- [16] E. Hamid, D. Moraru, J.C. Tarido, S. Miki, T. Mizuno, M. Tabe, *Appl. Phys. Lett.* 97/26 (2010) 262101.
- [17] M. Tabe, A. Udhiarto, D. Moraru, T. Mizuno, *Phys. Status Solidi A*, 208/3 (2011) 646.
- [18] A. Udhiarto, D. Moraru, T. Mizuno, M. Tabe, *Appl. Phys. Lett.* 99/11 (2011) 113108.
- [19] S. Petrosyan, A. Yesayan, D. Reuter, A.D. Wieck, *Appl. Phys. Lett.* 84/17 (2004) 3313.
- [20] D. Reuter, C. Werner, A.D. Wieck, S. Petrosyan, *Appl. Phys. Lett.* 86/16 (2005) 162110.
- [21] S.M. Sze, *Physics of Semiconductor Devices*, 2nd ed., John Wiley & Sons, 1981, p.754.
- [22] D.P. Foty, *Cryogenics*, 30/12 (1990) 1056.
- [23] M. Fischetti, S. Laux, *Phys. Rev. B*, 38/14 (1998) 9721.